International Journal of Electrical, Electronic and Communication Sciences
ISSN: 2517-9438
Vol:9, No:10, 2015

Design Modelling Control and Simulation of DC/DC Power Buck Converter

H. Abaali

***Abstract*—**The power buck converter is the most widely used DC/DC converter topology. They have a very large application area such as DC motor drives, photovoltaic power system which require fast transient responses and high efficiency over a wide range of load current. This work proposes, the modelling of DC/DC power buck converter using state-space averaging method and the current-mode control using a proportional-integral controller. The efficiency of the proposed model and control loop are evaluated with operating point changes. The simulation results proved the effectiveness of the linear model of DC/DC power buck converter.

***Keywords*—**DC/DC power buck converter, Linear current control, State-space averaging method.

NOMENCLATURE

C	Capacitance of the capacitor;
α	Duty cycle;
i_c	Capacitor current;
i_{in}	Input current;
i_L	Inductor current;
I_o	Output current (load current);
L	Inductance of the inductor;
R	Resistance of the load resistor;
T	Switching period;
f	Switching frequency;
V_e	Input voltage;
V_s	Output voltage;
V_{sref}	Output voltage reference;
v_k	Switching voltage;
v_D	Diode voltage;
V_c	Voltage control signal of Gate Turn-Off thyristor (GTO).

I. INTRODUCTION

THE DC/DC power buck converters convert high level DC voltage signal to low level stabilized DC voltage signal. They have received an increasing deal of interest in many areas. This is due to their high conversion efficiency and flexible output voltage. The DC/DC power buck converters are extensively used in the applications like appliance control such as DC motor drives, photovoltaic power system....

Due to the switching characteristics of the DC/DC power buck converter, the control problem poses a challenge for researchers. The objective of the switching control in DC/DC power buck converter is to realize high power transfer efficiency and good tracking of output voltage. Many control methods are used for control of switch mode DC/DC power buck converter and the simple and low cost controller structure is always in demand for most industrial applications [1]-[3]. The control method that gives the best performances under any conditions is always in demand. Conventionally, the DC/DC power buck converters have been controlled by linear voltage mode and current mode control methods such as proportional integral (PI) and proportional integral derivative (PID) controllers [4].

To obtain high performance control of converters, a good model of the converter should be designed. The DC/DC power buck converter modelling is described in [1]-[7].

In this paper, a linear approach for modelling and control of the DC/DC power converter are proposed. On the basis of the state-space averaging method, we calculated the output transfer function of power buck converter which can be further utilized for designing of a PI controller. The performance of the linear model and control loop are tested with operating point changes. The numerical simulations demonstrate the efficiency of proposed approach.

This paper is organized as following: after the introduction and short description of DC/DC power buck converter circuit, we present in the third section the components design and waveforms converter analysis. The fourth section gives the state-space averaging model of power buck converter. The fifth section presents a brief exposition of the PI linear control loop. In the sixth section, the simulation results and discussion are presented. Finally, the obtained results are commented in the last section.

II. POWER BUCK CONVERTER CIRCUIT TOPOLOGY

A large number of DC/DC converter circuits are known that can increase or decrease the magnitude of DC voltage and/or invert its polarity. Fig. 1 illustrates the power buck converter circuit topology.

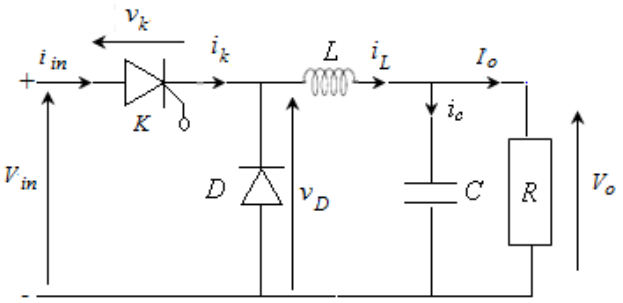

Fig. 1 Power buck converter circuit

The switch K is commonly realized using a power Gate

H. Abaali is with the Moulay Ismaïl University, Faculty of Sciences and techniques, BP 509 Boutalamine, Errachidia, Morocco (phone : +212 5 35 57 44 97; fax: +212 5 35 57 47 14; e-mail: habaali@gmail.com).

Turn-Off thyristor (GTO) and diode. However, other semiconductor switches such as Bipolar Transistor, Insulated Gate Bipolar Transistor (IGBT) and Metal–Oxide–Semiconductor Field-Effect Transistor (MOSFET), can be substituted if desired.

III. Components Design and Waveforms Power Buck Converter Analysis

To obtain the differential equations describing the power buck converter, we consider the ideal topology shown in Fig. 1. The system of differential equations describing the dynamics of the power buck converter is obtained through the direct application of Kirchoff's rules laws for each one of the possible circuit topologies arising from the assumed particular switch position function value.

A. Current and Voltage Components

During t_{on}: ($0<t<\alpha T$ (K: ON, D: OFF) $\alpha=t_{on}/T$

$v_k(t) \approx 0$, $i_{in}(t) = i_o(t)$, $i_D(t) = 0$ and $v_D(t) = -V_{in}$

$$V_o(t) = V_o = V_R + v_L(t) \text{ and } v_L(t) = L\frac{di_o(t)}{dt} \quad (1)$$

During t_{off} ($\alpha T <t<T$ (K:OFF, D: ON)

$$v_D(t) \approx 0,\ i_{in}(t) = 0$$

$$i_D(t) = i_L(t) \text{ and } V_R + v_L(t) = 0 \quad (2)$$

B. Differential Equations

During t_{on}

$$V_{in}(t) = V_o(t) + L\frac{di_L(t)}{dt} \quad (3)$$

The solution of (3) is given by:

$$i_L(t) = \frac{V_{in}(t) - V_o(t)}{L}t + i_L(0) \quad (4)$$

with $i_L(0) = I_{o\min}$

During t_{off}:

$$V_o(t) + L\frac{di_L(t)}{dt} = 0 \quad (5)$$

The solution of (5) is given by:

$$i_L(t) = \frac{-V_o(t)}{L}(t - \alpha T) + i_L(\alpha T) \quad (6)$$

with

$$i_L(\alpha T) = I_{o\max} = \frac{V_{in}(t) - V_o(t)}{L}\alpha T + I_{o\min}$$

C. Average Value of the Output Voltage and Output Current

$$V_o = \frac{1}{T}\int_0^{\alpha T} V_o(t)dt + \frac{1}{T}\int_{\alpha T}^{T} V_o(t)dt = \alpha V_{in} \quad (7)$$

with $V_o = \alpha V_{in} \le V_{in}$

$$I_o = \frac{1}{TR}\int_0^T V_o(t)dt = \alpha\frac{V_{in}}{R} = \frac{I_{o\max} + I_{o\min}}{2} \quad (8)$$

D. Output current Ripple

During t_{on}

The average value of (3) is given by:

$$V_{in} - V_o = L\frac{\Delta i_o}{\alpha T} = V_{in}(1-\alpha) \ge 0 \quad (9)$$

$\Rightarrow$ The current creases in the L.

During t_{off}

The average value of (5) is given by:

$$-V_o = L\frac{\Delta i_o}{(1-\alpha)T} \le 0 \quad (10)$$

$\Rightarrow$ The current decreases in L.

Finally, the output current ripple can be expressed by:

$$\Delta i_o = \frac{V_{in}}{Lf}(1-\alpha)\alpha = I_{o\max} - I_{o\min} \quad (11)$$

E. Average Value of the Input Current

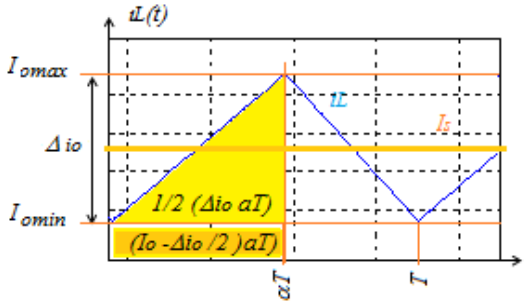

Fig. 2 Inductance current

Based on Fig. 2, the average value of the input current can be calculated by:

$$I_{in} = \frac{1}{T}\int_0^T i_{in}(t)dt = \alpha I_o \quad (12)$$

F. Output Voltage Ripple

The capacitor current, given by (13), is equivalent to the alternative component of output current given by:

$$i_C(t) = C\frac{dv_C(t)}{dt} = C\frac{dV_o(t)}{dt} \quad (13)$$

Assumed the switching frequency value is sufficiently high, the output current form is composed of straight portions. Consequently, the capacitor voltage (output voltage) is composed of parable portions:

$$V_o(t) = \frac{1}{C}\int i_C(t)dt \tag{14}$$

Fig. 3 shows the output voltage and the capacitor current.

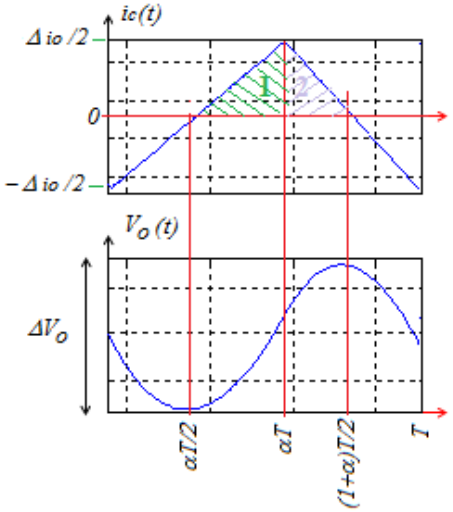

Fig. 3 Capacitor current and output voltage

V_{omin} and V_{omax} respectively corresponding to $\alpha T/2$ and $(1+\alpha)T/2$. The output voltage ripple can be calculated by:

$$\Delta V_o = \frac{1}{C}\int_{\alpha T/2}^{(1+\alpha)T/2} i_C(t)dt = \frac{\Delta i_o}{8Cf} \tag{14}$$

Replace the expression of the output current ripple given by (11) in (14). The output voltage ripple can be finally expressed by:

$$\Delta V_o = \frac{V_{in}}{8LCf^2}\alpha(1-\alpha) \tag{15}$$

G.LC Filter Design

The inductance and capacitor of *LC* filter can be designed using (11) and (15). The inductance should be designed considering the maximal value of output current ripple corresponding to $\alpha=0.5$. Thus, the output current ripple will never exceed the specified value:

$$L = \frac{V_{in}}{\Delta i_o f}(0,5)^2 \tag{16}$$

The switching frequency value can be increased to reduce the inductance value if sizing, based on the Δi_o, leads to excessive values. The output current ripple value decreases with the increase of the inductance or the switching frequency values.

In the steady state the waveforms power buck converter are given in Fig. 4.

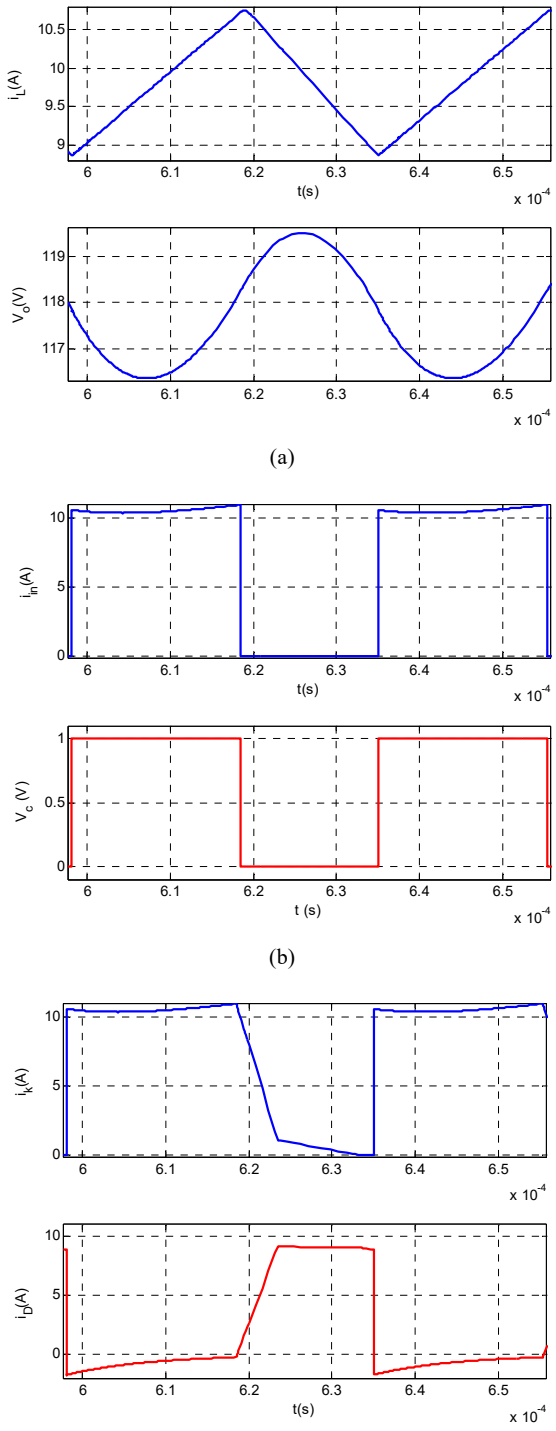

Fig. 4 (a) output current and output voltage, (b) input current and voltage control signal of GTO, (c) GTO and diode currents

IV. State-Space Averaging Model of Power Buck Converter

The DC/DC power buck converter can be described as switching between different time-invariant systems and is

subsequently a time-variant system. The state-space descriptions of the different time-invariant systems are used as a starting point in the state-space averaging method. The control-to-output transfer function can be obtained by applying the state-space averaging method to the DC/DC power buck converter [8].

The components of the DC/DC power buck converter are assumed ideal (equivalent circuit given in Fig. 1). The waveforms of the signals in the circuit are as shown in Fig. 4 and they are obtained from a matlab simulation. Steady state is reached and, therefore, the control signal $V_c(t)$, consists of pulses with constant width.

- While the thyristor is ON, the voltage across the diode is equal to the input voltage and the circuit in Fig. 5 (a) can be used as a model.
- While the thyristor is OFF, the voltage across the diode is equal to zero and the circuit in Fig. 5 (b) can be used as a model.

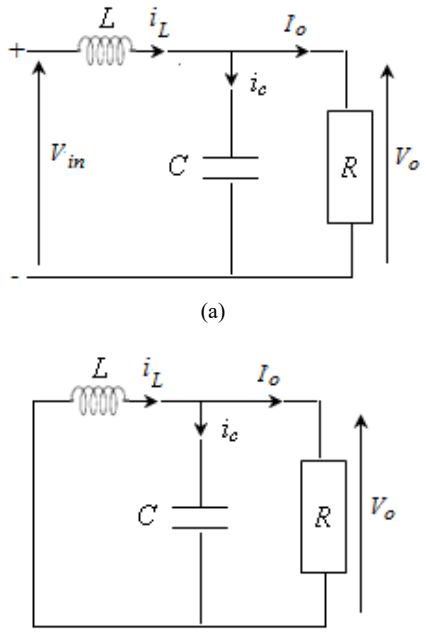

(a)

(b)

Fig. 5 The circuit of the DC/DC power buck converter: (a) switch ON during t_{on} and (b) switch OFF during t_{off}

The state-space descriptions of the circuits in Figs. 5 (a) and (b) are given in (17) and (18).

$$\begin{cases} \dfrac{dx(t)}{dt} = A_1 x(t) + B_1 u(t) \\ y(t) = C_1 x(t) + E_1 u(t) \end{cases} \tag{17}$$

$$\begin{cases} \dfrac{dx(t)}{dt} = A_2 x(t) + B_2 u(t) \\ y(t) = C_2 x(t) + E_2 u(t) \end{cases} \tag{18}$$

with:

$$x(t) = \begin{bmatrix} i_L(t) \\ V_s(t) \end{bmatrix},\ u(t) = \begin{bmatrix} V_{in}(t) \\ i_{in}(t) \end{bmatrix} \text{ and } y(t) = V_o(t) \tag{19}$$

The two systems are different linear time-invariant. In state-space averaging method, these two systems are first averaged with respect to their duration in the switching period:

$$\begin{cases} \dfrac{dx(t)}{dt} = [d(t)A_1 + (1-d(t))A_2]x(t) + [d(t)B_1 + (1-d(t))B_2]u(t) \\ y(t) = [d(t)C_1 + (1-d(t))C_2]x(t) + [d(t)E_1 + (1-d(t))E_2]u(t) \end{cases} \tag{20}$$

The system equation (20) is an approximation of the time-variant system and new variable names should formally have been used. To limit the number of variable names, this is not made. The duty cycle $d(t)$ is an additional input signal. A new input vector is therefore defined:

$$u'(t) = \begin{bmatrix} u(t) \\ d(t) \end{bmatrix} \tag{21}$$

This is not made in traditional presentations of state-space averaging, where the control signal $d(t)$ is kept separate from the disturbance signals $V_{in}(t)$ and $i_L(t)$. However, in system theory, all control signals and disturbance signals are put in an input vector.

Since the duty cycle can be considered to be a discrete-time signal with switching frequency f, one cannot expect the system in the last differential equation to be valid for frequencies higher than half the switching frequency.

The second step in state-space averaging method is linearization of the nonlinear time-invariant system. The deviations from an operating point are defined as:

$$x(t) = X + \hat{x}(t),\ u'(t) = U' + \hat{u}'(t),\ y(t) = Y + \hat{y}(t) \tag{22}$$

X, U' and Y denote the operating-point (DC, steady-state) values; $\hat{x}, \hat{u}'$ and $\hat{y}$ denotes the perturbation (AC) signals. The result is a linearized (AC, small-signal) system:

$$\begin{cases} \dfrac{d\hat{x}(t)}{dt} = A'\hat{x}(t) + B'\hat{u}'(t) \\ \hat{y}(t) = C'\hat{x}(t) + E'\hat{u}'(t) \end{cases} \tag{23}$$

Besides the AC model given in (23), a DC model can be obtained from (20) by setting the perturbation components to zero. One can extract the transfer function of power buck converter from the Laplace transform of (23).

$$H(p) = \frac{\hat{V}_o(p)}{\hat{d}(p)} = H_0 \frac{1}{1 + 2\dfrac{\xi}{\omega_n}p + \dfrac{p^2}{\omega_n^2}} \tag{24}$$

with

$$\omega_n = \frac{1}{\sqrt{LC}},\ \xi = \frac{\omega_n}{2}\frac{L}{R} \text{ and } H_0 = V_{in}$$

The operating-point value of $d(t)$ is denoted D and D'=1- D.

V. Current-Mode Control

In a current-mode control, an additional inner control loop is used as shown in Fig. 6, where the control voltage directly controls the output inductor current that feeds the output stage and thus the output voltage. Ideally, the control voltage should act to directly control the average value of the inductor for the faster response. The fact that the current feeding the output stage is controlled directly in a current-mode control has a profound effect on the dynamic behavior of the negative feedback control loop [4].

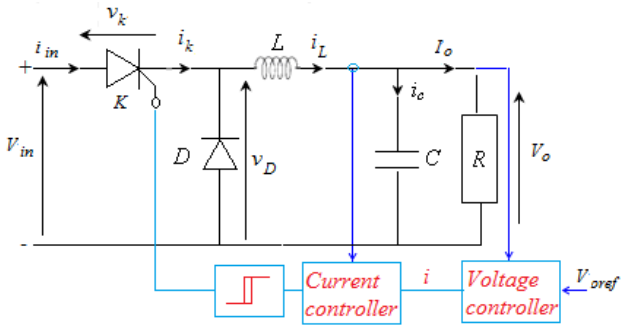

Fig. 6 The DC/DC power buck converter with a current controller and a voltage controller

VI. Simulation Results

The values of the capacitor and inductor will vary. In this paper, we consider an ideal DC/DC power buck converter, but they do provide us some rough values to start the designing and analysis of our system. All diode, thyristor and *LC* filter are ideal components, the input voltage is also a pure *DC* value; and the duty cycle remains approximately constant.

For an input voltage V_{in}= *209V*, output voltage V_o=*125.4V*, current ripple Δi_o=*5%*I_o and the voltage ripple ΔV_o=*2.68%* V_o:

The duty cycle is given by:

$$\alpha = \frac{V_o}{V_{in}} \approx 55\%$$

The output current can be calculated by:

$$I_o = \frac{I_{in}}{\alpha} = \frac{5{,}5}{0{,}55} \approx 10A$$

LC filer value can be calculated by:

$$L = \frac{V_{in}}{\Delta i_o f}(1-\alpha)\alpha \approx 1mH \text{ and } C = \frac{V_{in}}{8\Delta V_o L f^2}(1-\alpha)\alpha = 2.8\mu F$$

The simulation parameters are summered in Table I

Based upon these calculated values the corresponding open loop and closed Bode Plots are given in Figs. 7 and 8.

Fig. 9 depicts the dynamic response of the DC/DC power buck converter output voltage to the output voltage reference step change from 120V to 80V at 0.3ms and from 80V to 120V at 0.6ms.

TABLE I
The Simulation Parameter Values of the Power Buck Converter

Variable	Parameter	Value
L	Inductance	1mH
C	Output filter capacitance	2.8μF
V_{in}	Input voltage	210V
V_o	Out put voltage	115.5V
P_n	Constant power load	1.2kW
f	Switching frequency	27.4kHz
R	load	10Ω

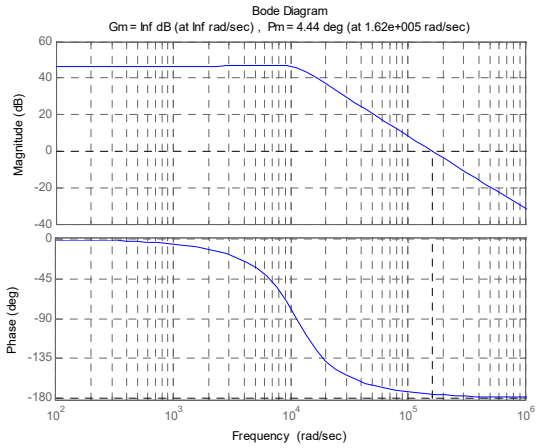

Fig. 7 Bode plot of DC/DC power buck converter transfer function

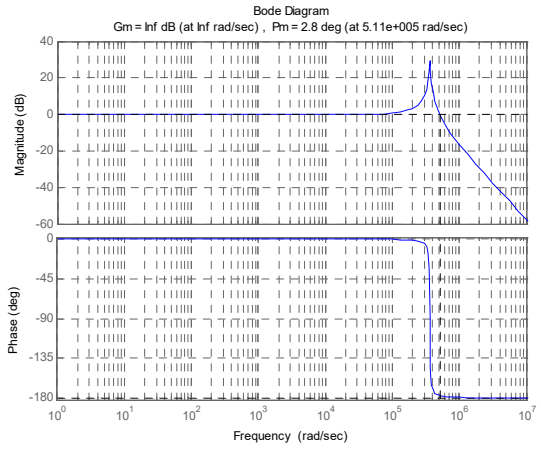

Fig. 8 Bode plot of DC/DC power buck converter closed loop transfer function

Fig. 10 shows the dynamic analysis of output inductance current i_L and output current I_o of feedback control of DC/DC power buck converter.

Fig. 11 shows the phase portrait. The reference voltage is 120V and the load is 10 Ω. The controller makes the trajectory to form a stable limit cycle. The limit cycle width on the V_o-axis is equal to the voltage ripple seen on the output of the converter. The two phases of the dynamics can easily be

observed. This is due to the fact that control input is not in infinite frequency.

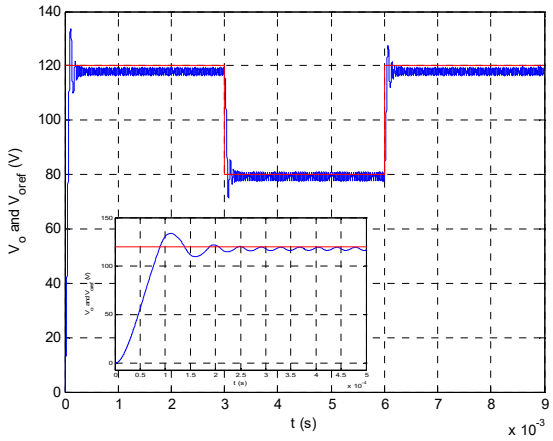

Fig. 9 Dynamic analysis of output voltage feedback control of DC/DC power buck converter

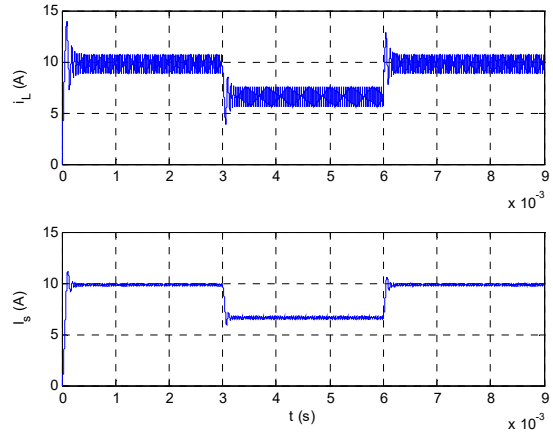

Fig. 10 Dynamic analysis of output inductance current i_L and output current I_o of feedback control of DC/DC power buck converter

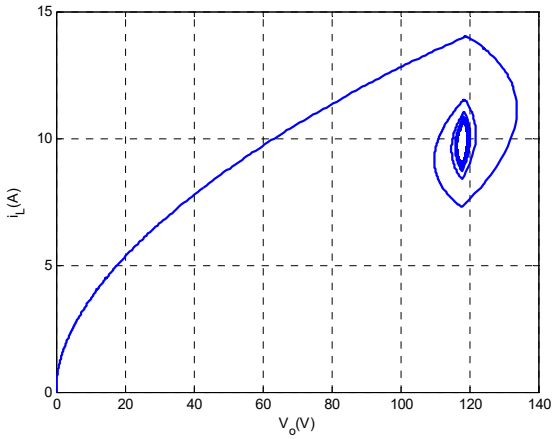

Fig. 11 Phase portrait (output voltage, current waveforms)

The step response characteristics of DC/DC power buck converter are summered in Table II.

TABLE II
STEP RESPONSE CHARACTERISTICS OF DC/DC POWER BUCK CONVERTER

Parameter	Value
Rise time	0.06ms
Settling time	0.98ms
Minimum value of y once the response has risen	107.33V
Maximum value of y once the response has risen	133.75V
Percentage overshoot (relative to output voltage final)	12.59V
Percentage undershoot	0
Peak absolute value of output volage	133.75V
Time at which this peak is reached	0.11ms

VII. CONCLUSION

In this paper, the linear model of DC/DC power buck converter is developed on the basis of the state-space averaging method. The output voltage of the power buck converter is regulated using a PI controller. The performance of the proposed model and control loop of DC/DC power buck converter are tested with operating point changes. The numerical simulations demonstrate the efficiency, offers a fast dynamic response and it is robust against the variations of the output voltage of DC/DC power buck converter.

In the future work, we will study the design, modelling, liner control of DC/DC real power buck converter considering the Equivalent Series Resistance (ESR) of the capacitor, the Resistance in the diode while it conducts, and the Resistance in the inductor.

REFERENCES

[1] Chi K. Tse and Keith M. Adams "Qasi-Linear Modeling and Control of DC-DC Convertres" IEEE Transactions on Power Electronics, Vol. 7, No. 2, April 1992
[2] A.J. Forsyth and S.V. Mollow, "Modeling and control of dc-dc converters," IEE power engineering journal, vol. 12, no. 5, pp. 229–236, Oct. 1998
[3] Bengt Johansson "DC-DC Converters -Dynamic Model Design and Experimental Verification" Theses Lund University SWEDEN 2004
[4] V.S.C Raviraj and P.C. Sen, "Comparative Study of proportional-integral, Sliding-mode, and fuzzy logic controllers for power converters," IEEE transaction on Industry applications, vol. 33, no. 2, pp. 518-524, Mar. /Apr. 1997
[5] Alireza Khaligh, Ali Emadi "Stabilizing Control of DC/DC Buck Converters with Constant Power Loads in Continuous Conduction and Discontinuous Conduction Modes Using Digital Power Alignment Technique Journal of Electrical Engineering & Technology, Vol. 1, NO. 1, pp. 63-72, 2006
[6] Loïc Michel, Cédric Join, Michel Fliess, Pierre Sicard and Ahmed CH´E RITI "Model-free control of dc/dc converters" Author manuscript, published in "12th IEEE Workshop on Control and Modeling for Power Electronics (COMPEL2010) inria-00495776, version 1 - 29 Jun 2010
[7] Yungtaek Jang, Milan M. Jovanovic "Bridgeless High-Power-Factor Buck Converter" IEEE Transactions on Power Electronics, Vol. 26, NO. 2, Februry 2011
[8] R.D. Middlebrook And Slobodan Cuk "A General Unified Approach To Modelling Switching-Converter Power Stages" Reprinted, vith permission, from Proceedings of the IEEE Power Electronics Specialists Conference, June 8-10, 1976

LHoussine Abaali was born on 10 October, 1974 in Khenifra, Morrocco. He received his B.S. degree in 1995, the L.S. degree in 1999, the Extensive graduate diploma (DESA/Masters) from the Cady University, Faculty of Science Semlalia in 2001 and the Dr degree in Power Electronic and electrical engineering from Cady University, Faculty of Science Semlalia in 2007. From 2007 to 2009, he was a professor at the Higher Technician Certificate (BTS) at the Laayoune Centre Morocco. He is currently Professor of electrical engineering at the Moulay Ismaïl University, Faculty of sciences and techniques, Errachidia, Morocco. His research interests are Electrical Power Distribution, Operations, Planning, Management, and Simulation of Electric Energy Systems, Power System Quality.